LAB. INVESTIGATION-HUMAN/ANIMAL TISSUE

Retinoids induced astrocytic differentiation with down regulation of telomerase activity and enhanced sensitivity to taxol for apoptosis in human glioblastoma T98G and U87MG cells

Arabinda Das · Naren L. Banik · Swapan K. Ray

Abstract We hypothesized that induction of differentiation with retinoid could increase sensitivity to microtubule-binding drug taxol (TXL) for apoptosis in human glioblastoma T98G and U87MG cells. Treatment of cells with 1 μM all-*trans* retinoic acid (ATRA) or 1 μM 13-*cis* retinoic acid (13-CRA) for 7 days induced astrocytic differentiation, overexpression of glial fibrillary acidic protein (GFAP), and also down regulated telomerase expression and activity, thereby increased sensitivity to TXL for apoptosis. Treatment of glioblastoma cells with TXL triggered production of reactive oxygen species (ROS), induced phosphorylation of p38 mitogen-activated protein kinase (MAPK), and activated the redox-sensitive c-Jun NH_2-terminal kinase 1 (JNK1) pathway. Moreover, TXL activated Raf-1 kinase for phosphorylation and inactivaion of anti-apoptotic Bcl-2 protein. The events of apoptosis included increase in expression of Bax, down regulation of Bcl-2 and baculoviral inhibitor-of-apoptosis protein (IAP) repeat containing (BIRC) proteins, mitochondrial release of cytochrome c and Smac into the cytosol, increase in intracellular free $[Ca^{2+}]$, and activation of calpain, caspase-9, and caspase-3. Increased activity of caspase-3 cleaved inhibitor of caspase-activated DNase (ICAD) to release and translocate CAD to the nucleus for DNA fragmentation. Involvement of stress signaling kinases and proteolytic activities of calpain and caspase-3 in apoptosis was confirmed by pretreating cells with specific inhibitors. Taken together, our results suggested that retinoid (ATRA or 13-CRA) induced astrocytic differentiation with down regulation of telomerase activity to increase sensitivity to TXL to enhance apoptosis in glioblastoma cells. Thus, combination of retinoid and TXL could be an effective therapeutic strategy for controlling the growth of glioblastoma.

Keywords Apoptosis · Cysteine proteases · Differentiation · Glioblastoma · Retinoid · Taxol

Abbreviations

ANOVA	Analysis of variance
Asc	Ascorbic acid
ATRA	All-*trans* retinoic acid
BIRC	Baculovirus IAP repeat containing
CAD	Caspase-3-activated DNase
13-CRA	13-*cis* Retinoic acid
DMSO	Dimethyl sulfoxide
HRP	Horseradish peroxidase
hTERT	Human telomerase reverse transcriptase (hTERT)
IAP	Inhibitor-of-apoptosis protein
ICAD	Inhibitor of caspase-3-activated DNase
K_d	Dissociation constant
MAPK	Mitogen-activated protein kinase
p-NA	p-Nitroanilide
OD	Optical density
ROS	Reactive oxygen species
RT-PCR	Reverse transcription-polymerase chain reaction
SBDP	Spectrin breakdown product
TXL	Taxol
SB203580	4-(4-Fluorophenyl)-2-(4-methylsulfinyl phenyl)-5-(4-pyridyl)-1H-imidazole

A. Das · N. L. Banik · S. K. Ray (✉)
Division of Neurology, Department of Neurosciences, Medical University of South Carolina (MUSC), 96 Jonathan Lucas Street, Suite 325E, P.O. Box 250606, Charleston, SC 29425, USA
e-mail: raysk@musc.edu

Introduction

Apoptosis is the mechanism of cell death in cancer cells treated with taxol (TXL), which is a plant-derived anti-cancer agent [1]. This has been confirmed in leukemia cells, ovarian carcinoma cells, gastric carcinoma cells, head-and-neck tumors, prostate tumors, adrenocortical carcinoma cells, and even in glioblastoma cells [1]. Glioblastoma is the most prevalent and malignant brain tumor in humans. However, the biochemical events that TXL triggers leading to apoptosis in glioblastoma cells are not well understood. Because current treatment of glioblastoma patients with TXL alone is ineffective, innovative therapeutic strategies are needed for treating this deadly disease. In the present study, we have tried to develop a dual approach to control the growth of glioblastoma by promoting differentiation with a retinoid and enhancing apoptosis with TXL.

Retinoids, retinoic acid and its derivatives, are highly regarded for their efficacy as differentiating agents and are effective in the treatment of promyelocytic leukemia and neuroblastoma, but they show only moderate effects on glioblastoma [2]. Induction of differentiation by retinoid is associated with down regulation of telomerase activity [2], which otherwise maintains telomeric length and fuels unlimited proliferation of cancer cells. A stereoisomer of all-*trans* retinoic acid (ATRA) is 13-*cis* retinoic acid (13-CRA), which has shown anti-tumor activity in the treatment of hematologic and solid malignancies [3]. Retinoids, which are effective in the treatment of promyelocytic leukemia and neuroblastoma [3], have been used for treating glioblastoma with only moderate effects. However, retinoids in some cases are highly effective in combination with another therapy. For example, combination of 13-CRA with TXL or cisplatin and/or IFN-α has entered Phase I and II clinical trials for the treatment of head-and-neck carcinoma, squamous cell carcinoma, non-small cell lung carcinoma, renal cell carcinoma, and prostate tumor [4, 5]. These observations prompted us to analyze the efficacy of combination of a retinoid with TXL in human glioblastoma T98G and U87MG cells.

The cytotoxic effect of TXL is generally attributed to its anti-microtubule activity and also Bcl-2 phosphorylation, leading to apoptosis in cancer cells. Multiple mechanisms are likely to be involved in mediation of apoptosis by TXL. Many agents, which are not themselves oxidants, may cause significant increase in intracellular reactive oxygen species (ROS) for induction of apoptosis [5]. Moreover, some inducers of apoptosis may activate the mitogen-activated protein kinase (MAPK) pathway. However, the role of MAPK pathway in inducing apoptosis in glioblastoma following treatment with TXL is not entirely clear. It should be noted here that although the activation of p38

MAPK is generally associated with induction of apoptosis, activation of p42/44 MAPK exerts cytoprotective effects [6]. Recently, we reported activation p38 MAPK pathway in glioblastoma cells following treatment with plant-derived compounds [7].

Our current investigation indicated that retinoid induced differentiation and down regulated telomerase activity in T98G and U87MG cells to increase sensitivity to TXL for apoptosis via multiple mechanisms with the involvement of stress kinases and cysteine proteases.

Matetials and methods

Cell culture

Both T98G and U87MG cells were grown in 75-cm^2 flasks each containing 10 ml of RPMI 1640 (Sigma Chemical, St. Louis, MO, USA), 1% penicillin and streptomycin (GIBCO, Grand Island, NY, USA), and 10% fetal bovine serum (FBS) (GIBCO). Both ATRA and 13-CRA (Sigma Chemical) were dissolved in dimethyl sulfoxide (DMSO) and stored as 1000x stock aliquots at −70°C. Prior to any treatment, cells were allowed to grow in RPMI 1640 in presence of 0.5% FBS for 24 h. Glioblastoma cells were treated with 1 μM ATRA or 13-CRA for 7 days for induction of astrocytic differentiation. Since the retinoids are sensitive to light, all treatments involving retinoids were performed under subdued lighting. Each experiment included control cultures that received the same amount of DMSO that was used in the retinoid treatment. The concentration of DMSO in each experiment was always less than or equal to 0.01%, which was not toxic and did not induce differentiation. For induction of apoptosis, cells were treated with 0.1 μM TXL (Sigma Chemical) for 24 h. For all incubations, cells were kept in a 37°C incubator with full humidity and 5% CO$_2$. After all treatments, cells were processed for evaluation of biochemical basis for induction of differentiation and apoptosis.

Methylene blue staining for detection of morphological features of astrocytic differentiation

Glioblastoma T98G and U87MG cells were cultured in monolayer in 9-cm diameter plates in absence and presence of 1 μM ATRA or 13-CRA for 7 days. Culture medium was aspirated and washed twice with ice-cold PBS, pH 7.4. Each plate was placed on ice and 5 ml of ice-cold 50% (v/v) ethanol was added to fix the cells. Ethanol was aspirated followed by the addition of 5 ml of ice-cold 0.2% (w/v) methylene blue solution (made up in 50% ethanol). Cells were stained for 30 s, washed twice with ice-cold water,

and the plates were dried in the air. Cells were examined under the light microscope at $400\times$ magnification.

Trypan blue dye exclusion test for determination of residual cell viability

Following treatments, the residual viability in the attached and detached cell populations was estimated by trypan blue dye exclusion test [8–10]. At least 600 cells were counted in four different fields and the percentage of residual cell viability was calculated.

Wright staining for morphological features of apoptosis and ApopTag assay for biochemical evidence of apoptosis

Glioblastoma T98G and U87MG cells from each treatment were detached with a cell-scraper to harvest attached and detached cells together. Cells were washed twice in PBS and sedimented onto the microscopic slide using an Eppendorf 5804R centrifuge (Brinkmann Instruments, Westbury, NY, USA) at $106\times g$ for 5 min. Cells were fixed and then subjected to Wright staining and ApopTag assay [8–10]. Cellular morphology was examined by light microscopy to assess apoptosis. At least 800 cells were counted in each treatment, and the percentage of apoptotic cells was calculated.

Telomeric repeat amplification protocol (TRAP) assay for determination of telomerase activity

Telomerase activity was determined by application of the TRAP assay [11] with some modifications. Briefly, cells were washed once with ice-cold PBS, and again with ice-cold wash buffer. Cells were lysed in ice-cold lysis buffer for 30 min on ice, and centrifuged in a microfuge at 4°C. The supernatant was removed and used immediately or quick frozen on dry-ice. The protein concentration in the supernatant was measured by Coomassie Brilliant Blue assay (Pierce, Rockford, IL, USA). Assay tubes were prepared by sequestering 0.2 μg of CX primer (5'-CC CTT ACC CTT ACC CTT ACC CTT AA-3') under a wax barrier known as Ampliwax (Cetus Corporation, Emeryville, CA, USA). In each TRAP assay tube, 150 ng of protein was used in 50 μl of reaction mixture containing 20 mM Tris-HCl, pH 8.3, 1.5 mM $MgCl_2$, 63 mM KCl, 1 mM EGTA, 0.1 mg/ml bovine serum albumin, 0.005% (v/v) Tween-20, 1 ag/μl Internal Telomerase Assay Standard (ITAS), 0.2 μg TS primer (5'-AA TCC GTC GAG CAG AGT T-3'), 1 μg T4g32 protein (Roche Applied

Science, IN, USA), and 2.5 units *Taq* DNA polymerase (Roche Applied Science). After 30 min of incubation at 23°C for telomerase-mediated extension of the TS primer, the reaction mixture was heated at 90°C for 3 min and then subjected to polymerase chain reaction (PCR) for 35 cycles (programming of each cycle: 94°C for 45 sec, 50°C for 45 sec, and 72°C for 1 min). The PCR products were electrophoresed on 12% polyacrylamide gels, stained with 1 μg/ml ethidium bromide, destained the background in water, examined on a UV transilluminator at 303 nm, and photographed.

Detection of reactive oxygen species

The fluorescent probe 2',7'-dichlorofluorescein diacetate (DCF-DA) was used for the assessment of intracellular ROS production in T98G and U87MG cells. This is a widely-used method for the measurement of intracellular ROS such as hydrogen peroxide (H_2O_2), hydroxyl radical, and hydroperoxides [12]. Briefly, cells were seeded (1×10^5 cells/well) in 6-well culture plates. Next day, cells were washed twice with Hank's balanced salt solution (HBSS) (GIBCO) and loaded with 500 μl HBSS containing 5 μM DCF-DA and 0.1 μM TXL. Cells were then incubated at 37°C for 30 to 150 min and the fluorescence intensity was measured at 530 nm after excitation at 480 nm in Spectramax Gemini XPS (Molecular Devices, Sunnyvale, CA, USA). The increase in fluorescence intensity was used to assess the generation of net intracellular ROS.

Fura-2 assay for determination of intracellular free $[Ca^{2+}]$

Levels of intracellular free $[Ca^{2+}]$ were measured in T98G and U87MG cells using the fluorescence Ca^{2+} indicator fura-2/AM, as we described previously [8–10]. The value of K_d, a cell-specific constant, was determined experimentally to be 0.387 μM for the T98G cells and 0.476 μM for the U87MG cells, using standards of the Calcium Calibration Buffer Kit with Magnesium (Molecular Probes, Eugene, OR, USA).

Analysis of mRNA expression

Extraction of total RNA, reverse transcription-polymerase chain reaction (RT-PCR), and agarose gel electrophoresis were performed as we described previously [13]. All primers (Table 1) for the RT-PCR experiments were designed using the Oligo software (National Biosciences,

Plymouth, MN, USA). The level of β-actin gene expression served as an internal control.

Antibodies

Monoclonal IgG antibody against α-spectrin (Affiniti, Exeter, UK) was used to measure calpain activity as well as caspase-3 activity. Bax and Bcl-2 monoclonal IgG antibodies (Santa Cruz Biotechnology, Santa Cruz, CA, USA) were used to assess regulation of apoptotic death. Also, IgG antibodies against phosphorylated-Thr56-Bcl-2 (p-Bcl-2), JNK1, phosphorylated-Thr183-JNK1 (p-JNK1), p38 MAPK, and phosphorylated-Tyr18-p38 MAPK (p-p38 MAPK) were obtained from Santa Cruz Biotechnology. Monoclonal IgG antibody against β-actin (clone AC-15, Sigma Chemical) was used to standardize protein loading on the SDS-PAGE. The secondary antibody used was horseradish peroxidase (HRP)-conjugated goat anti-mouse IgG (ICN Biomedicals, aurora, OH, USA) except in the case of calpain and α-spectrin where we used HRP-conjugated goat anti-rabbit IgG (ICN Biomedicals).

Western blotting

Western blotting was performed, as we described previously [8–10]. The autoradiograms were scanned using Photoshop software (Adobe Systems, Seattle, WA, USA) and optical density (OD) of each band was determined using the Quantity One software (Bio-Rad, Hercules, CA, USA).

Measurement of mitochondrial membrane potential

We measured the changes in mitochondrial membrane potential ($\Delta\psi_m$) in T98G and U87MG cells using the J aggregate-forming lipophilic cationic dye JC-1 [14]. Control cells and cells for TXL treatment were incubated in medium containing 5 µg/ml JC-1 during drug treatments for 1–24 h. After being stained, the cells were washed twice with PBS and resuspended in PBS. Cells were excited at 488 nm and the fluorescence emission of JC-1 was measured in a fluorescent plate reader (Molecular Devices, Sunnyvale, CA, USA) at wavelengths

Table 1 Primers used for determining levels of mRNA expression of specific genes

Gene	Primer sequence	Product size (bp)
β-actin	Sense: 5′-GTG GGG CGC CCC AGG CAC CA-3′	436
	Antisense: 5′-CTC CTT AAT GTC ACG CAC GAT TTC-3′	
bax	Sense: 5′- GCA GGG AGG ATG GCT GGG GAG A-3′	352
	Antisense: 5′-TCC AGA CAA GCA GCC GCT CAC G-3′	
bcl-2	Sense: 5′-CCG GGA GAT CGT GAT GAA GTA-3′	708
	Antisense: 5′-CAT ATT TGT TTG GGG CAT GTC T-3′	
BIRC-2	Sense: 5′-CAG AAA GGA GTC TTG CTC GTG-3′	536
	Antisense: 5′-CCG GTG TTC TGA CAT AGC ATC-3′	
BIRC-3	Sense: 5′-GGG AAC CGA AGG ATA ATG CT-3′	368
	Antisense: 5′-ACT GGC TTG AAC TTG ACG GAT-3′	
BIRC-4	Sense: 5′-AAT GCT GCT TTG GAT GAC CTG-3′	470
	Antisense: 5′-ACC TGT ACT CAG CAG GTA CTG-3′	
BIRC-5	Sense: 5′-GCC CCA CTG AGA ACG-3′	302
	Antisense: 5′-CCA GAG GCC TCA ATC C-3′	
BIRC-6	Sense: 5′-AGC CGA AGG ATA GCG A-3′	385
	Antisense: 5′-GCC ATC CGC CTT AGA A-3′	
BIRC-7	Sense: 5′-GCC TCC TTC TAT GAC T-3'	283
	Antisense: 5'-CGT CTT CCG GTT CT-3'	
BIRC-8	Sense: 5′-GTG AGC GCT CAG AAA GAC ACT AC-3′	209
	Antisense: 5'-CAC ATG GGA CAT CTG TCA ACT G-3'	
GFAP	Sense: 5′-CGC CTC GAT CAA CTC A-3′	210 [24]
	Antisense: 5′-CTC CTC CAG CGA CTC AAT-3′	
hTERT	Sense: 5′-GTA CAT GCG ACA GTT C-3′	418 [25]
	Antisense: 5′-TTC TAC AGG GAA GTT CAC-3′	
hTER	Sense: 5′-TCT AAC CCT AAC TGA GAA GGG CGT AG-3′	126 [26]
	Antisense: 5′-GTT TGC TCT AGA ATG AAC GGT GGA AG-3′	

corresponding to its monomer (530 ± 15 nm) and J aggregate (>590 nm) forms. Any decrease in the JC-1 monomer:J aggregate ratio indicated a drop in $\Delta\psi_m$ in the cells.

Preparations and analyses of cytosolic, mitochondrial, and nuclear protein fractions

Preparations of cytosolic, mitochondrial, and nuclear protein fractions were performed by standard procedures [10]. Cytochrome c in the supernatants and pellets and also CAD in nuclear fractions were analyzed by Western blotting.

Colorimetric assays for measurement of caspase-9 and caspase-3 activities

Measurements of caspase-9 and caspase-3 activities in cells were performed with the commercially available assay kits (Sigma Chemical). Proteolytic activities of caspase-9 and caspase-3 were assayed based on the release of p-nitroanilide (p-NA) from LEHD-p-NA and DEVD-p-NA, respectively. The concentration of the p-NA released from the substrate was calculated from the absorbance at 405 nm.

Treatment with specific inhibitors for prevention of cell death

Cells were pretreated (1 h) with Ascorbic acid (Asc), JNK inhibitor I, p38 MAPK inhibitor (SB203580), calpeptin, caspase-9 inhibitor I, or caspase-3 inhibitor IV (Calbiochem) at 10 μM. Control cultures were pretreated (1 h) with an equivalent amount of DMSO (≤0.1%) or left untreated. The inhibitor was used to pretreat the cells before addition of TXL and maintained throughout the experiment. Lower concentrations of the inhibitor did not show significant inhibition of cell death and higher concentrations were toxic. After the treatments, the residual cell viability was calculated based on the trypan blue dye exclusion test.

Statistical analysis

All results obtained from different treatments of T98G and U87MG cells were analyzed using the StatView software (Abacus Concepts, Berkeley, CA, USA). Data were expressed as mean $\pm$ standard deviation (SD) of separate experiments ($n \geq 3$) and compared by one-way analysis of variance (ANOVA) followed by Fisher's post hoc test.

Significant difference between control and a treatment was indicated by * $P < 0.05$ or ** $P < 0.01$.
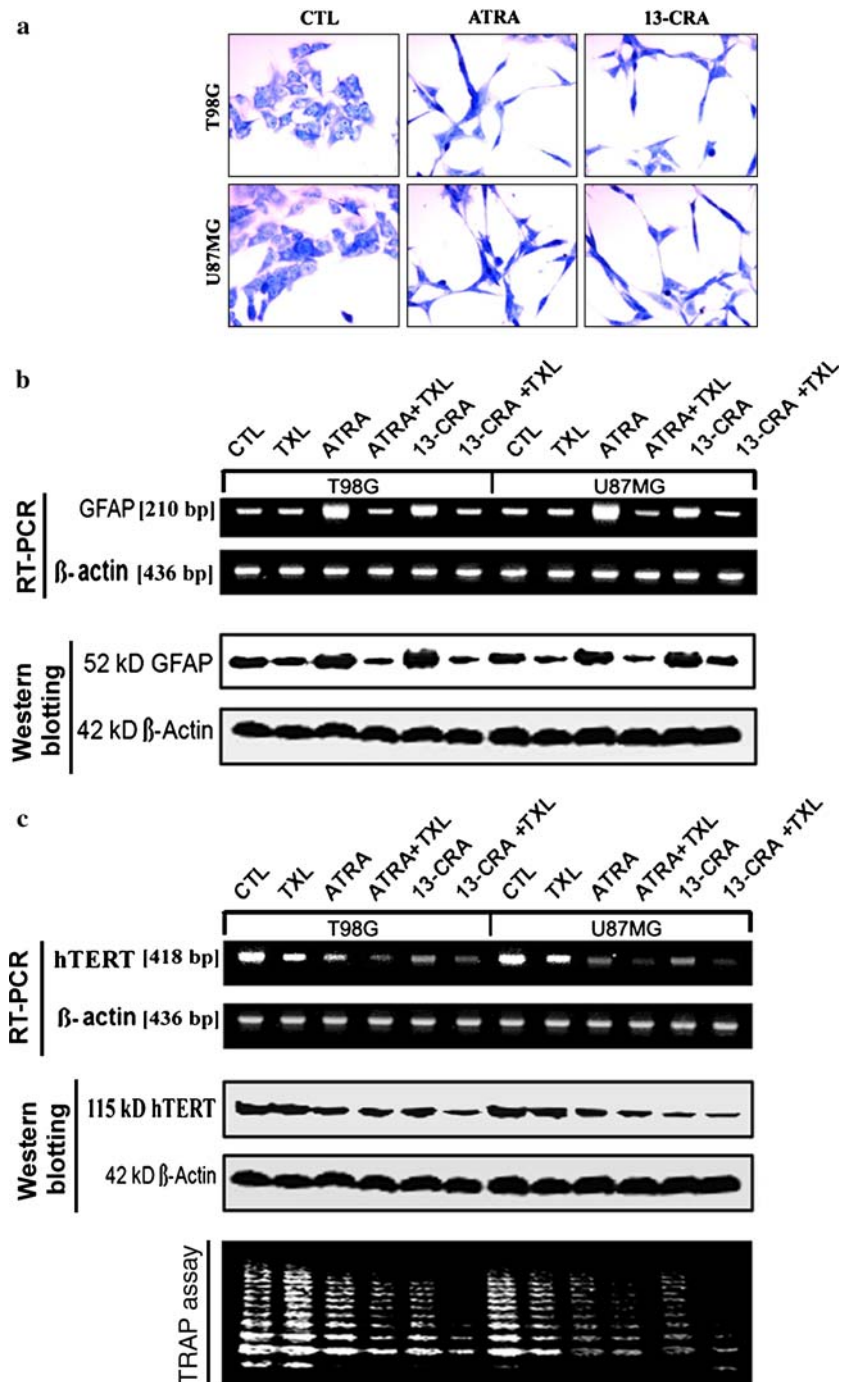
Results

Retinoids induced astrocytic differentiation with down regulation of telomerase activity in glioblastoma cells

We monitored the morphological and biochemical features of astrocytic differentiation in T98G and U87MG cells (Fig. 1). Both ATRA and 13-CRA induced morphological features of astrocytic differentiation (Fig. 1a). Since GFAP is a determining factor for astrocytic cell shape [15], the morphological alterations leading to differentiation observed may have occurred due to overexpression of GFAP. We observed overexpression of GFAP (2 folds or more) in differentiated cells, compared with control T98G and U87MG cells (Fig. 1b). Induction of differentiation was also associated with a decrease in expression of hTERT (as evaluated by the RT-PCR and Western blotting) and telomerase activity (as evaluated by the TRAP assay) in T98G and U87MG cells (Fig. 1c). In RT-PCR experiments, we did not detect any notable changes in level of human telomerase RNA (hTER) gene expression after treatments (data not shown). These results demonstrated that both ATRA and 13-CRA were capable of inducing astrocytic differentiation with overexpression of GFAP and down regulation of telomerase in both T98G and U87MG cells.

Retinoids sensitized glioblastoma cells to TXL for increasing apoptosis

Wright staining and ApopTag assay were employed to examine, respectively, morphological and biochemical features of apoptosis in glioblastoma cells (Fig. 2). Wright staining showed characteristic morphological features of apoptosis (Fig. 2a) while ApopTag assay detected DNA fragmentation in cells undergoing apoptotic death (Fig. 2b). In ApopTag assay, control (CTL) cells showed little or no brown color, confirming almost absence of apoptosis. Percentage of apoptosis was determined based on ApopTag assay (Fig. 2c). Compared with CTL cells, treatment of cells with 0.1 μM TXL for 24 h showed an increase in the percentage of apoptotic cells, whereas treatment of cells with ATRA or 13-CRA alone did not induce apoptosis. But pretreatmentnt of both T98G and U87MG cells with retinoids highly increased sensitivity to TXL for apoptosis. Thus, Wright staining and ApopTag assay clearly demonstrated the sensitization of differentiated T98G and U87MG

Fig. 1 Astrocytic differentiation with overexpression of GFAP and down regulation of telomerase activity in T98G and U87MG cells. (**a**) Methylene blue staining for morphological features of astrocytic differentiation. Three treatment (7 days) groups: control (CTL); 1 μM ATRA; 1 μM 13-CRA. (**b**) Examination of changes in GFAP expression at the mRNA (RT-PCR) and protein (Western blotting) levels after different treatments. (**c**) Detection of changes in hTERT at mRNA (RT-PCR) and protein (Western blotting) levels and changes in telomerase activity (**TRAP assay**) after different treatments. Treatment groups (in panels **b** and **c**): CTL; 0.1 μM TXL (24 h); 1 μM ATRA (7 days); 1 μM ATRA (7 days) + 0.1 μM TXL (24 h); 1 μM 13-CRA (7 days); and 1 μM 13-CRA (7 days) + 0.1 μM TXL (24 h)
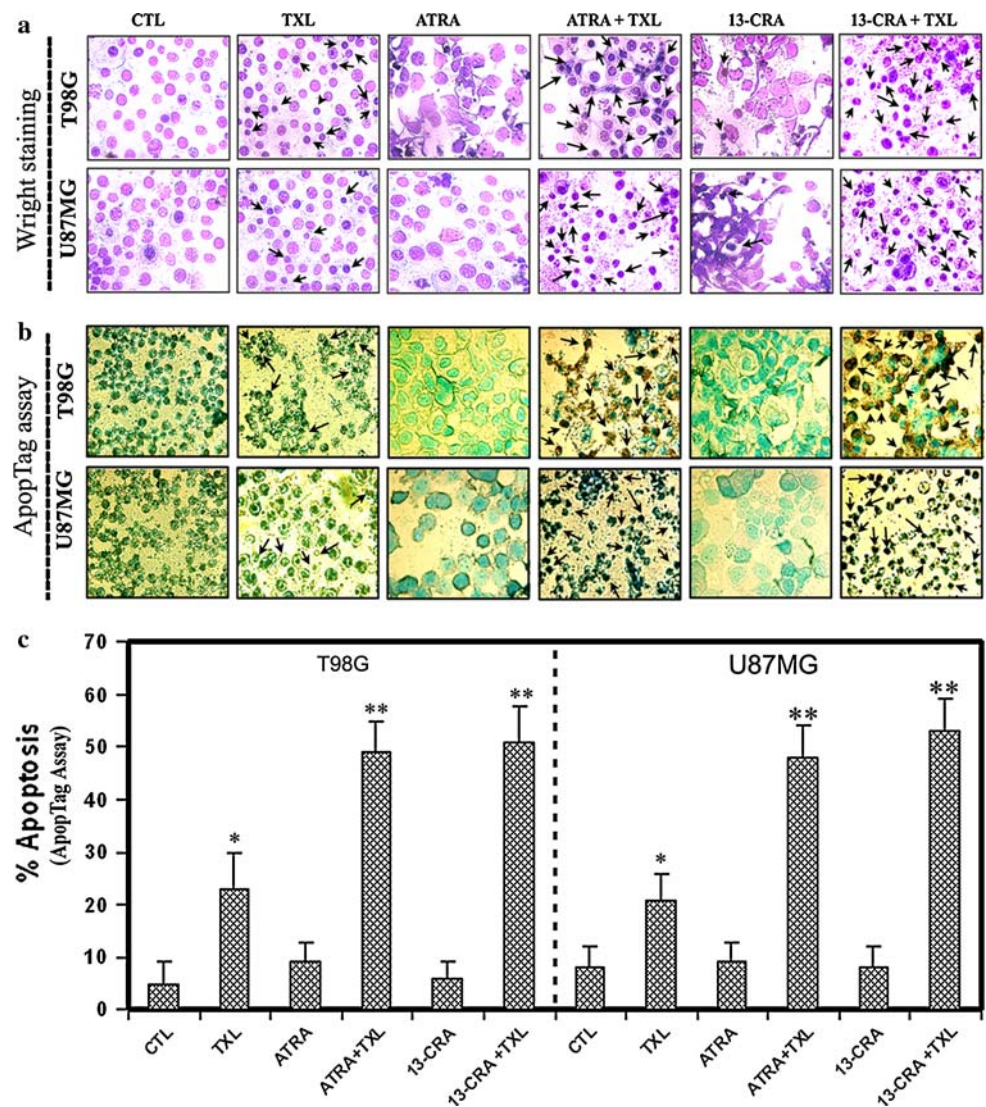

cells to TXL for increasing morphological and biochemical features of apoptotosis.

TXL induced ROS production and p38 MAPK phosphorylation to cause apoptosis

We examined the possibility of ROS production and p38 MAPK phosphorylation (p-p38 MAPK) in glioblastoma cells (Fig. 3). To investigate the ROS production for apoptosis in T98G and U87MG cells, we monitored the oxidation of DCF-DA as a measure of ROS production [16]. An increase in ROS production could increase intracellular free $[Ca^{2+}]$ in glioblastoma cells [7]. Time-dependently, TXL promoted the oxidation of DCF-DA indicating the ROS production in T98G cells as well as in U87MG cells (Fig. 3a). We did not see any significant change in ROS production in control and other treatments (data not shown). Pretreatment of cells with Asc completely blocked an increase in ROS production and TXL

Fig. 2 Detection of morphological and biochemical features of apoptosis in T98G and U87MG cells. (**a**) Wright staining for morphological features of of apoptosis. (**b**) ApopTag assay for detecting DNA fragmentation in apoptotic cells. (**c**) Bar diagram to show percent apoptosis based on ApopTag assay. Treatment groups (in panels **a**, **b**, and **c**): CTL; 0.1 μM TXL (24 h); 1 μM ATRA (7 days); 1 μM ATRA (7 days) + 0.1 μM TXL (24 h); 1 μM 13-CRA (7 days); and 1 μM 13-CRA (7 days) + 0.1 μM TXL (24 h)

mediated apoptosis indicating that TXL promoted ROS production for apoptosis in T98G and U87MG cells. To determine whether activation of p38 MAPK (i.e., formation of p-p38 MAPK) was required for induction of apoptosis, we examined the effect of the selective p-p38 MAPK inhibitor (SB203580) that showed no inhibitory action on p44/42-MAPK and c-JNK [17]. Our results showed that p38 MAPK activation occurred following TXL treatment of cells (Fig. 3b,c). Pretreatment of cells with 10 μM Asc or 2 μM SB203580 almost completely blocked cell death (Table 2). The ROS scavenger Asc completely blocked the phosphorylation of p38 MAPK in T98G cells as well as in U87MG cells (Fig. 3d), suggesting the involvement of ROS in TXL mediated phosphorylation of p38 MAPK. Taken together, these results indicated that TXL induced ROS production and p38 MAPK phosphorylation for mediation of apoptosis in glioblastoma cells.

TXL activated Raf-1 kinase for Bcl-2 phosphorylation and also activated JNK1

In response to various treatments, there exists a possibility of phosphorylation of Bcl-2 (p-Bcl-2). Whether this phosphorylation activates or inactivates the anti-apoptotic function of Bcl-2 may depend on cell type or treatment itself. Furthermore, multiple kinases have been proposed to mediate the phosphorylation of Bcl-2 in response to various treatments [18]. We found that treatment of glioblastoma cells with TXL induced phosphorylation of Raf-1 (p-Raf-1) for its activation (Fig. 4). Recent studies have shown that TXL leads to activation of Raf-1 and this activation is essential for formation of p-Bcl-2 (i.e., inactivation) and apoptosis [19]. In the present study, we demonstrated that TXL induced phosphorylation of Raf-1 as well as of Bcl-2. Western blotting showed an increase in phosphorylation of JNK1 (p-JNK1) for its activation
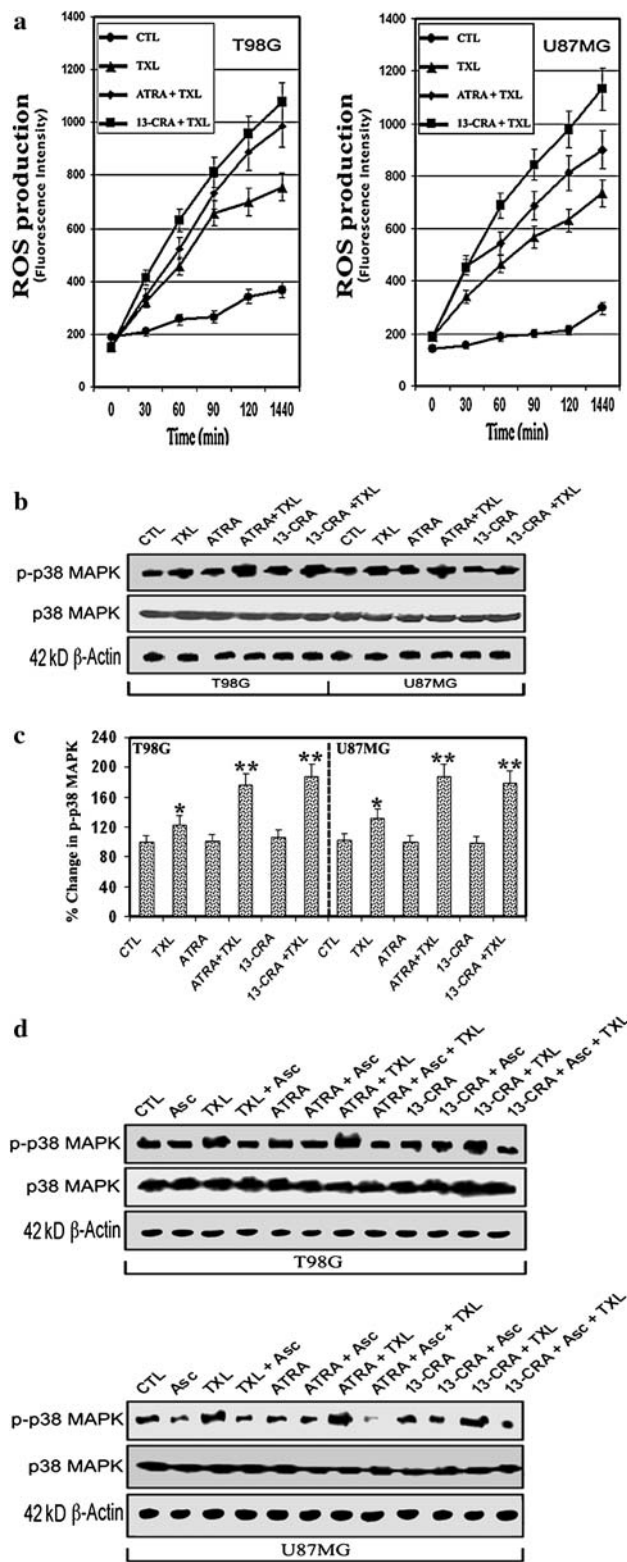
◀ **Fig. 3** Increase in ROS production induced activation of p38 MAPK in T98G and U87MG cells. Treatment with TXL increased production of ROS in T98G and U87MG cells. (**a**) Treatment groups: 0.1 μM TXL, 1 μM ATRA (7 days) + 0.1 μM TXL, 1 μM 13-CRA (7 days) + 0.1 μM TXL. Cells were treated with 0.1 μM TXL (for 0, 30, 60, 90, 120, 150, and 1440 min) in presence of 5 μM DCF-DA. It should be noted that cells in CTL, 1 μM ATRA, and 1 μM 13-CRA treatment groups as well as in Asc pretreatment groups did not show any increase in ROS production (data not shown). (**b**) Representative Western blots to show levels of p-p38 MAPK, p38 MAPK, and β-actin. (**c**) Bar diagram to show percent changes in p-p38 MAPK over control. Treatment groups (in panels **b** and **c**): CTL; 0.1 μM TXL (24 h); 1 μM ATRA (7 days); 1 μM ATRA (7 days) + 0.1 μM TXL (24 h); 1 μM 13-CRA (7 days); and 1 μM 13-CRA (7 days) + 0.1 μM TXL (24 h). (**d**) Pretreatment of cells with Asc prevented phosphorylation of p38 MAPK. Treatment groups: CTL; 10 μM Asc (24 h); 0.1 μM TXL (24 h); 10 μM Asc (1-h pretreat) + 0.1 μM TXL (24 h); 1 μM ATRA (7 days); 1 μM ATRA (7 days) + 10 μM Asc (24 h); 1 μM ATRA (7 days) + 0.1 μM TXL (24 h); 1 μM ATRA (7 days) + 10 μM Asc (1-h pretreat) + 0.1 μM TXL (24 h); 1 μM 13-CRA (7 days); 1 μM 13-CRA (7 days) + 10 μM Asc (24 h); 1 μM 13-CRA (7 days) + 0.1 μM TXL (24 h); and 1 μM 13-CRA (7 days) + 10 μM Asc (1-h pretreat) + 0.1 μM TXL (24 h)

in our experiments using cell-permeable JNK inhibitor I. Pretreatment of cells with 10 μM JNK inhibitor I protected cells from TXL mediated cell death (Table 2), indicating the involvement of JNK1 pathway in cell death.

Involvement of mitochondria and mitochondrial factors in mediation of cell death

We examined changes in expression of pro-apoptotic Bax and anti-apoptotic Bcl-2 levels leading alteration in mitochondrial permeability for releasing mitochondrial factors for activation of mitochondria-dependent caspase cascade (Fig. 5). Examination of mRNA expression by RT-PCR experiments showed that TXL treatment increased bax levels and decreased bcl-2 levels while β-actin levels remained uniform in all treatments (Fig. 5a). A monoclonal antibody recognized 21 kD Bax α and 24 kD Baxβ isoforms and another antibody for detected 26 kD Bcl-2 on the Western blots (Fig. 5a). β-Actin expression was monitored on the Western blots to ensure that equal amount of protein was loaded in each lane. Treatment of cells with TXL or combination of retinoid and TXL increased total Bax expression and decreased Bcl-2 expression (Fig. 5a) resulting in increase in Bax:Bcl-2 ratio (data not shown) to promote mitochondrial release of pro-apoptotic factors. Mitochondrial permeability may be increased with the loss of mitochondrial membrane potential ($\Delta\psi_m$), which is readily measured by staining mitochondria with the fluorescence dye JC-1 [14]. After treatments of cells with TXL or combination of retinoid and TXL, the mean red and green fluorescence ratio of the mitochondria dropped

following treatment of cells with TXL (Fig. 4). Notably, p-JNK1 regulates the transcription of several genes that can contribute to cell death. The involvement of activated JNK1 pathway in TXL mediated cell death was confirmed

Table 2 Pretreatment of cells with specific inhibitors prevented cell death

| Pretreatment	% Viability of T98G cells						% Viability of U87MG cells					
	CTL	TXL	ATRA	ATRA + TXL	13-CRA	13-CRA + TXL	CTL	TXL	ATRA	ATRA + TXL	13-CRA	13-CRA + TXL
None	94 ± 2.3	70 ± 4.3	93.3 ± 1.2	46.7 ± 0.6	92 ± 1.5	42.6 ± 3.2	93 ± 2.5	70 ± 2.6	92 ± 3.2	50 ± 4.6	90 ± 3.1	44.6 ± 4.0
Asc	91.6 ± 2.5	88 ± 5.2	91 ± 6.5	89.3 ± 2.1	91.7 ± 3.8	88.3 ± 3.8	90.7 ± 3.5	85 ± 7.8	90.7 ± 5.7	90 ± 2.6	86.3 ± 7.4	87.3 ± 6.0
SB203580	91.6 ± 2.5	88 ± 6.1	91 ± 6.5	84.6 ± 8.1	90.3 ± 3.8	90.3 ± 3.5	90.1 ± 3.5	86.7 ± 6.0	90.3 ± 5.7	88 ± 3.6	88.3 ± 6.4	90.3 ± 6.0
JNK inhibitor I	90.8 ± 5.5	89 ± 7.1	93 ± 2.5	89.6 ± 3.1	91.3 ± 3.9	91.3 ± 3.5	93.1 ± 2.6	88.7 ± 4.0	91.3 ± 2.7	90.7 ± 3.6	92.3 ± 4.4	92.3 ± 0.8
Calpeptin	92 ± 3.6	93.3 ± 1.2	95 ± 4.6	90.6 ± 2.5	92.6 ± 5.5	91.6 ± 4.6	90.6 ± 3.5	90.6 ± 3.8	89.3 ± 2	91.7 ± 3.1	91 ± 2.6	91 ± 3.4
Caspase-9 inhibitor I	93.6 ± 4.0	79 ± 1.5	89.0 ± 8.5	74 ± 4.0	96 ± 2.6	72 ± 4.7	90 ± 1.0	73.3 ± 4.0	94 ± 4.0	72.6 ± 3.0	89 ± 3.0	74.6 ± 5.0
Caspase-3 inhibitor IV	91.7 ± 5.6	90.7 ± 5.6	92.3 ± 6.3	90.3 ± 8.5	93.6 ± 4.1	91.0 ± 4.0	93.0 ± 4.0	91 ± 2.6	92.7 ± 2.1	92.7 ± 4.5	92.6 ± 1.5	91.6 ± 5.6
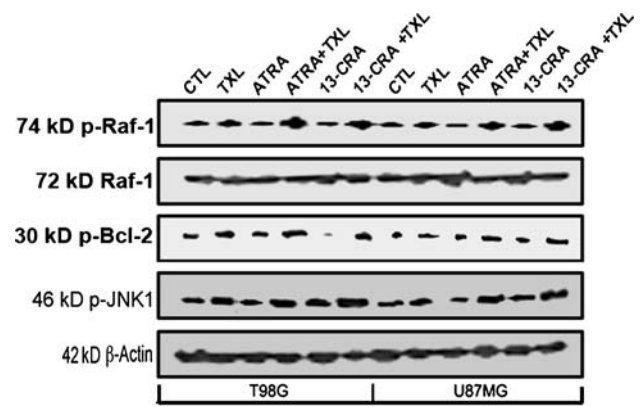
Fig. 4 Western blotting to examine phosphorylation of Raf-1, Bcl-2, and JNK1 in T98G and U87MG cells. Representative Western blots to show levels of p-Raf-1, Raf-1, p-Bcl-2, p-JNK1, and β-actin. Treatment groups: CTL; 0.1 µM TXL (24 h); 1 µM ATRA (7 days); 1 µM ATRA (7 days) + 0.1 µM TXL (24 h); 1 µM 13-CRA (7 days); and 1 µM 13-CRA (7 days) + 0.1 µM TXL (24 h)

slowly, indicating the loss of $\Delta\psi_m$ during apoptosis (Fig. 5b). We did not see any significant loss of $\Delta\psi_m$ in control and other treatments (data not shown). This loss of $\Delta\psi_m$ was associated with the disappearance of 15 kD cytochrome c from the mitochondria and its concurrent appearance in the cytosol (Fig. 5c). As an internal control, we monitored expression of COX4 in mitochondrial fraction whereas β-actin expression in cytosolic fraction. The mitochondrial release of cytochrome c into the cytosol could cause activation of caspase-9. Treatments with TXL or combination of retinoid and TXL increased active 37 kD caspase-9 fragment as detected by Western blotting (Fig. 5c) and also increased caspase-9 activity as determined by colorimetric assay (Fig. 5d). Pretreatment of cells with caspase-9 inhibitor I showed some inhibitory effect on cell death (Table 2). Taken together, these results suggested that increase in pro-apoptotic Bax expression was correlated to $\Delta\psi_m$ collapse for mitochondrial release of cytochrome c into the cytosol and subsequent activation of caspase-9.

Mitochondrial release of Smac into the cytosol and suppression of BIRC expression

In response to apoptotic stimuli, mitochondria may also release Smac into the cytosol to block function of inhibitor-of-apoptosis proteins (IAPs), which are endogenous inhibitors for prevention of activation of caspases [20]. Because all IAPs bear one or more characteristic zinc-finger motifs termed baculoviral IAP repeats (BIRs), the whole family of these proteins is now more precisely known as BIR containing (or BIRC) proteins rather than IAPs [20]. We used RT-PCR experiments to examine
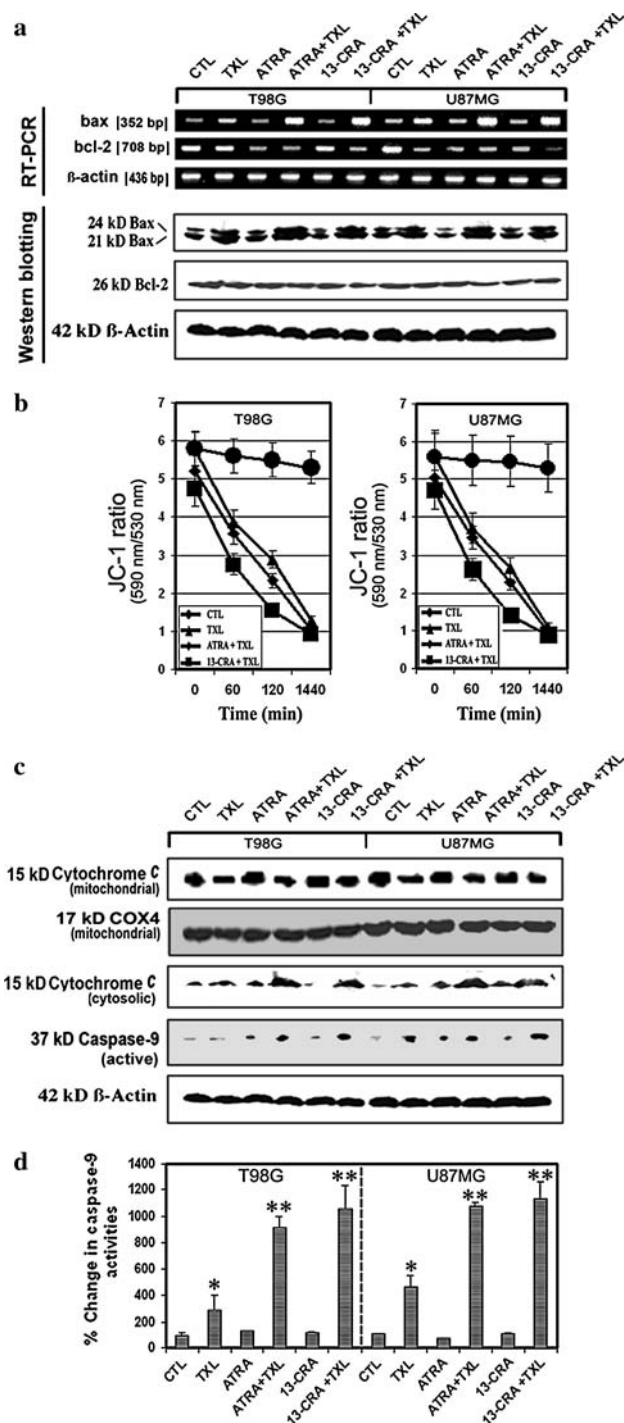
◀ **Fig. 5** An increase in Bax expression changed mitochondrial permeability to trigger activation of mitochondria-dependent caspase cascade in T98G and U87MG cells. (**a**) Representative pictures to show levels of Bax, Bcl-2, and β-actin at mRNA (RT-PCR) and protein (Western blotting) levels after different treatments. (**b**) Decrease in JC-1 monomer (590 nm):J aggregate (530 nm) ratio after treatments indicated loss of $\Delta\psi_m$ in glioblastoma cells. Treament groups: 0.1 μM TXL, 1 μM ATRA (7 days) + 0.1 μM TXL; and 1 μM 13-CRA (7 days) + 0.1 μM TXL. Cells were treated with TXL for 0, 60, 120, and 1440 min. Cells in CTL, 1 μM ATRA, and 1 μM 13-CRA treatment groups did not show change in $\Delta\psi_m$ (data not shown). (**c**) Representative Western blots to show levels of cytochrome *c*, COX4, active caspase-9, and β-actin. (**d**) Colorimetric assay for determination of caspase-9 activity. Treatment groups (in panels **a**, **c**, and **d**): CTL; 0.1 μM TXL (24 h); 1 μM ATRA (7 days); 1 μM ATRA (7 days) + 0.1 μM TXL (24 h); 1 μM 13-CRA (7 days); and 1 μM 13-CRA (7 days) + 0.1 μM TXL (24 h)

that TXL, most notably combination of retinoid and TXL, triggered mitochondrial release of Smac into the cytosol so as to down regulate BIRC proteins (Fig. 6b). We determined the down regulation of BIRC-3 (Fig. 6c) and BIRC-4 (Fig. 6d) following treatments. Thus, mitochondrial release of Smac into the cytosol correlated well with the suppression of selective BIRC proteins to promote activation of caspases.

Increase in intracellular free [Ca²⁺] and activation of calpain and caspase-3 for proteolysis

Increase in intracellular [Ca²⁺] could activate the Ca²⁺-dependent protease calpain. Increased proteolytic activities of both calpain and caspase-3 would indicate the demise of glioblastoma cells. Therefore, we examined the changes in intracellular free [Ca²⁺], activation of both calpain and caspase-3, and their proteolytic activities after the treatments of glioblastoma cells (Fig. 7). We determined the intracellular free [Ca²⁺] in the cells using the fura-2 assay [8–10]. Compared with CTL cells, treatments of cells with TXL and especially combination of retinoid and TXL caused significant increases in intracellular free [Ca²⁺] (Fig. 7a) suggesting the possibility of activation of calpain in course of cell death. Subsequently, Western blotting showed increase in active calpain fragment and degradation of calpastatin (endogenous calapin inhibitor) and also increase in active caspase-3 fragment very prominently following treatment of cells with combination of retinoid and TXL (Fig. 7b). Because high level of calpastatin prevented calpain mediated proteolysis [21], a decrease in calpastatin level could promote proteolytic activity of calpain. We detected increases in calpain and caspase-3 activities in proteolysis of 270 kD α-spectrin to generate calpain-specific 145 kD spectrin breakdown product (SBDP) and caspase-3-specific 120 kD SBDP, respectively (Fig. 7b). Further, we performed colorimetric assay to

alterations in mRNA expression of BIRC-2 to BIRC-8 and Western blotting to monitor mitochondrial release of Smac into the cytosol leading to down regulation of BIRC proteins (Fig. 6). Results from RT-PCR experiments showed that TXL, especially combination of retinoid and TXL, dramatically decreased mRNA expression of BIRC-2 to BIRC-6 in both T98G and U87MG cells (Fig. 6a). Levels of mRNA expression of BIRC-7 and BIRC-8 remained relatively unchanged (Fig. 6a). Western blotting showed
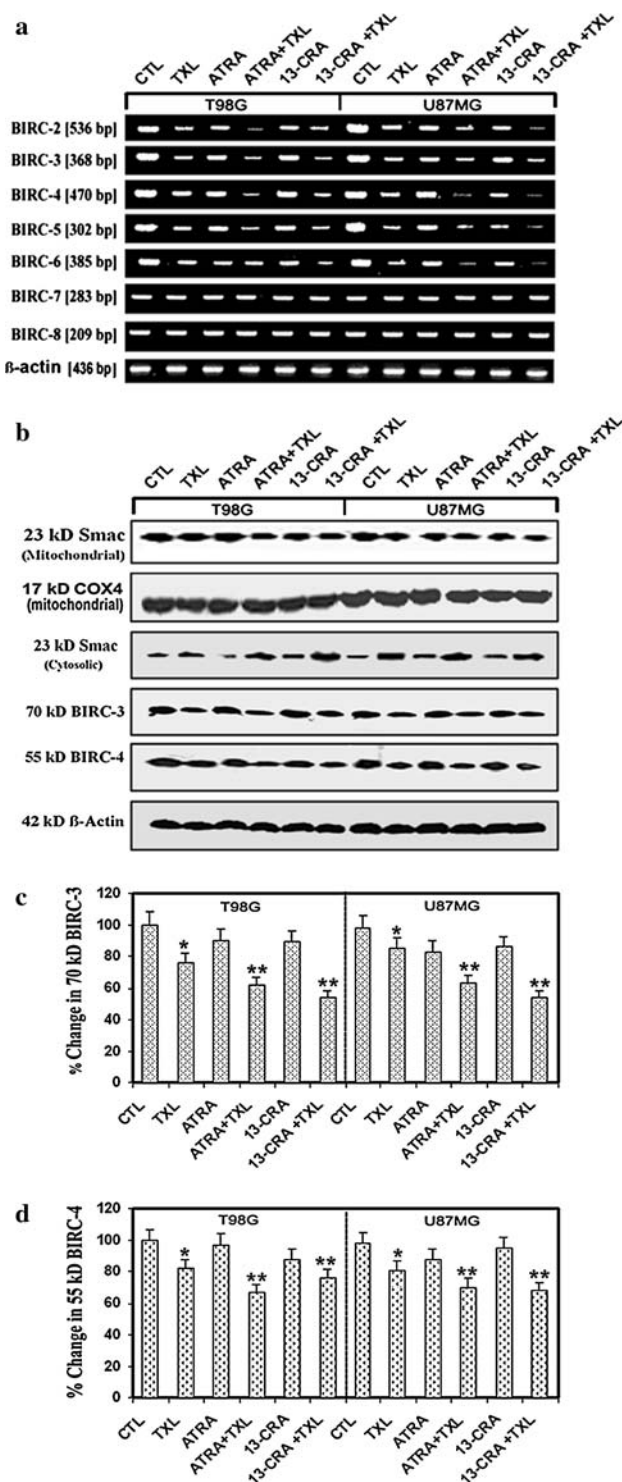
Fig. 6 Examination of changes in BIRC expression at mRNA level and mitochondrial release of Smac to down regulate selective BIRC proteins in T98G and U87MG cells. (**a**) Representative gel pictures to show mRNA levels of BIRC-2 to BIRC-8 and also β-actin. (**b**) Representative Western blots to show protein levels of Smac, COX4, BIRC-3, BIRC-4, and β-actin. Bar diagram to show percent changes in BIRC-3 (**c**) and BIRC-4 (**d**) at protein levels. Treatment groups: CTL; 0.1 μM TXL (24 h); 1 μM ATRA (7 days); 1 μM ATRA (7 days) + 0.1 μM TXL (24 h); 1 μM 13-CRA (7 days); and 1 μM 13-CRA (7 days) + 0.1 μM TXL (24 h)

demonstrate significant increases in caspase-3 activity in the cells treated with TXL and also combination of retinoid and TXL (Fig. 7c). Besides, increase in caspase-3 activity was correlated with the decrease in cytosolic level of 45 kD inhibitor of caspase-3-activated DNase (ICAD) so as to release and translocate 40 kD CAD to the nucleus (Fig. 7D) for nuclear DNA fragmentation. We used staining of total protein in nuclear fraction as loading control (Fig. 7d).

Based on our results, we proposed that treatment of glioblastoma cells with TXL and most notably combination of a retinoid (ATRA or 13-CRA) and TXL triggered ROS production leading to activation of stress kinases (p38 MAPK and JNK1), inactivation of Bcl-2, mitochondrial release of pro-apoptotic molecules, increase in intracellular free $[Ca^{2+}]$, and proteolytic activities of calpain and caspase-3 for apoptosis (Fig. 8).

Discussion

Chemotherapy with a single agent may be limited due to both toxicity and lack of potency. Therefore, combination chemotherapeutic strategies are currently being explored to reduce toxicity and enhance therapeutic efficacy. In this investigation, we explored the therapeutic efficacy of combination of a differentiation agent (ATRA or 13-CRA) and an anti-cancer agent (TXL) for controlling growth of glioblastoma. The strategy for induction of differentiation followed by activation of apoptosis has been found highly promising in cancer therapy (22). Our current results imply that differentiation with down regulation of telomerase activity has the potential to sensitize glioblastoma cells to TXL for increasing the amount of apoptosis. Our results provided direct evidence for down regulation of telomerase and overexpression of GFAP during differentiation in T98G and U87MG cells (Fig. 1). Apoptosis occurred (Fig. 2) due to production of ROS, which triggered phosphorylation of p38 MAPK (Fig. 3) as well as of Raf-1, Bcl-2, and JNK1 (Fig. 4). Besides, apoptosis was associated with increases in Bax level, loss of $\Delta \psi_m$, mitochondrial release of cytochrome c and activation of caspase-9 (Fig. 5), mitochondrial release of Smac and down regulation of BIRC proteins (Fig. 6), increase in intracellular free $[Ca^{2+}]$, and activation of calpain and caspase-3 (Fig. 7). We proposed a schematic diagram to show how combination of a retinoid (ATRA or 13-CRA) and TXL caused molecular alterations leading to differentiation and apoptosis in human glioblastoma cells (Fig. 8).

Our results suggested that astrocytic differentiation with down regulation of telomerase activity (Fig. 1) increased sensitivity of glioblastoma cells to TXL for apoptosis (Fig. 2). Accumulating evidence now suggests that ROS
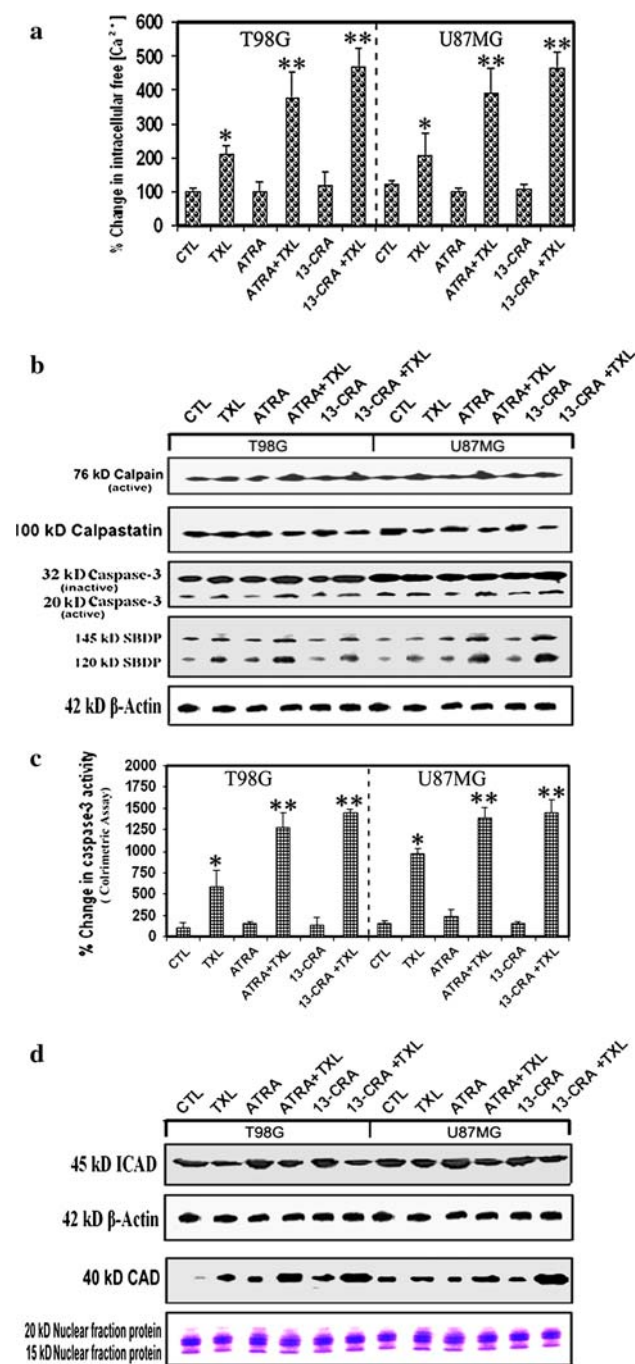
Fig. 7 Increase in intracellular free [Ca^{2+}] and activation of calpain and caspase-3 for protelysis in T98G and U87MG cells. Treatment groups (in panels A and B): CTL; 0.1 μM TXL (24 h); 1 μM ATRA (7 days); 1 μM ATRA (7 days) + 0.1 μM TXL (24 h); 1 μM 13-CRA (7 days); and 1 μM 13-CRA (7 days) + 0.1 μM TXL (24 h). (**a**) Determination of percent increase in intracellular free [Ca^{2+}] using fura-2 assay. (**b**) Representative Western blots to show levels of calpain, calpastain, caspase-3, SBDP, and β-actin. (**c**) Colorimetric assay for determination of caspase-3 activity. (**d**) Representative Western blots to show levels of ICAD and β-actin in the cytosolic fraction and CAD in nuclear fraction. A representative SDS-PAGE gel picture (stained with methylene blue) to show loading of equal amount of nuclear protein in each lane

may play a role in signaling apoptosis [5]. In our study, we found that TXL alone and combination of retinoid and TXL induced ROS production (Fig. 3). Pretreatment of cells with Asc decreased both ROS production and cell death, indicating a role for ROS in cell death. We also detected phosphorylation of p38 MAPK in course of apoptosis (Fig. 3). A decrease in phosphorylation of p38 MAPK due to pretreatment of cells with its specific inhibitor (SB203580) markedly decreased cell death (Table 2). Pretreatment with Asc completely blocked phosphorylation of p38 MAPK, suggesting a role for ROS in phosphorylation of p38 MAPK (Fig. 3). Also, the JNK1 pathway was activated in cell death because cell death was inhibited in the presence of cell-permeable JNK inhibitor I (Table 2), a synthetic peptide capable of specifically blocking JNK1 phosphorylation. Thus, we showed an essential role played by JNK1 pathway for cell death. Tubulin-modifying agents induce phosphorylation of Raf-1 and Bcl-2 and also JNK1 signaling for apoptosis [23]. We found that combination of retinoid (ATRA or 13-CRA) and TXL effectively induced phosphorylation of Raf-1 and Bcl-2 and activated JNK1 pathway for apoptosis in glioblastoma cells (Fig. 4).

Pro-apoptotic and anti-apoptotic members of the Bcl-2 family regulate the release of cytochrome c from the mitochondrial intermembrane space into the cytosol [12]. Cytochrome c then interacts with the pro-caspase-9 and Apaf-1 to activate caspase-9 to switch on caspase-3 activity leading to apoptosis [12]. So, we examined the levels of Bax and Bcl-2 and found an increase in Bax expression (Fig. 5) and mitochondrial release of cytochrome c and activation of caspase-9 in glioblastoma cells (Fig. 5). Smac was also released from mitochondria for promoting apoptosis in gliobalstoma cells (Fig. 6). The inhibitory effects of various BIRC proteins on apoptosis have been examined in different cell culture models [20]. Because Smac could suppress survival effects of BIRC proteins, we examined changes in the levels of BIRC proteins (Fig. 6) and found down regulation of BIRC-3 and BIRC-4 to promote apoptosis.

An increase in intracellular free [Ca^{2+}] is known to cause apoptosis [7–9]. Increases in intracellular free [Ca^{2+}] in glioblastoma cells following treatment with TXL or combination of retinoid and TXL (Fig. 7) suggested that activation of Ca^{2+}-dependent pathway was required for induction of apoptosis. We observed activation of the Ca^{2+}-dependent protease calpain, down regulation of calpastatin, increases in proteolytic activities of calpain and caspase-3, ICAD fragmentaion to release and translocate CAD to the nucleus (Fig. 7). We used protease inhibitors to confirm occurrence of cell death with activation of calpain, caspase-9, and caspase-3 (Table 2). Based on results, we

Fig. 8 A schematic diagram to show that combination of retinoid (ATRA or 13-CRA) and TXL induced differentiation and apoptotis in glioblastoma cells with activatiom of multiple molecular mechanisms. Arrows show direction of events and also upregulation or down regulation of the molecular events. Solid-block lines indicate inhibition of the molecular events. Treatment of cells with retinoid (ATRA or 13-CRA) alone induced astrocytic differentiation with upregulation of GFAP and down regulation of both hTERT expression and telomerase activity. Combination of retinoid and TXL worked synergistically to increase the amount of apoptosis due to ROS production and increase in intracellular free [Ca^{2+}] leading to activation stress kinases and proteolytic activities of calpain and caspases
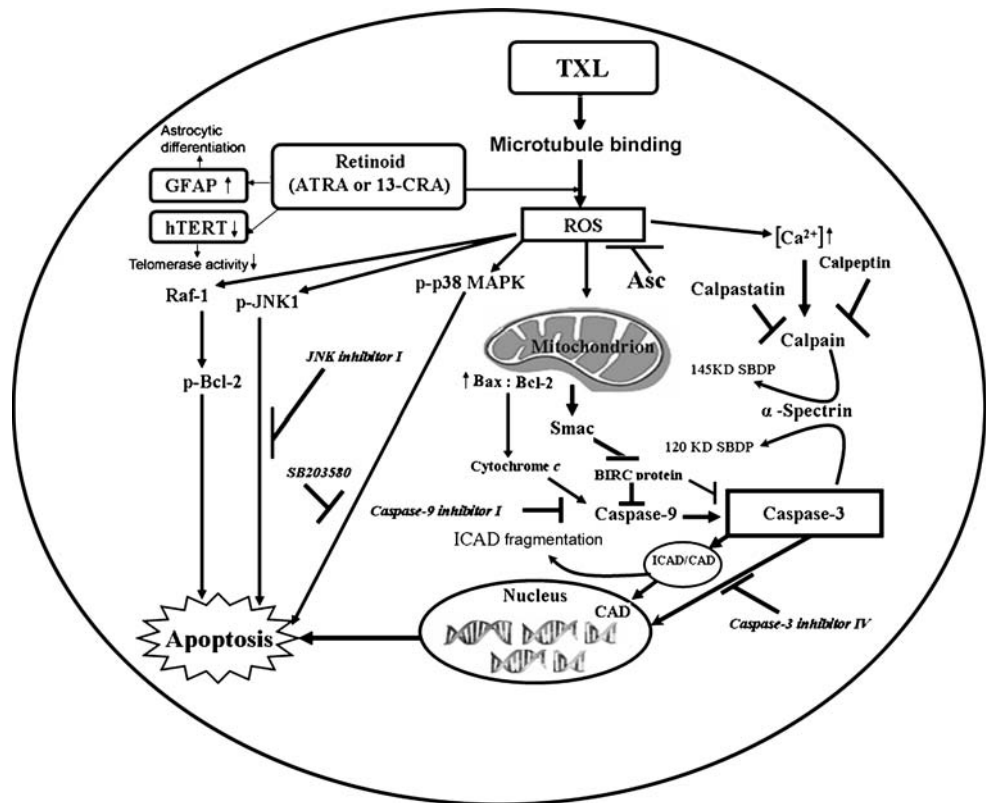
proposed that multiple pathways were involved for induction of differentiation and apoptosis in glioblastoma cells (Fig. 8). Combination of retinoid and TXL induced apoptosis in both T98G (mutant p53) and U87MG (wild-type p53) cells, indicating that this therapeutic strategy did not absolutely require functional p53 for inducing apoptosis.

In conclusion, combination of retinoid (ATRA or 13-CRA) and TXL effectively induced differentiation and apoptosis in human glioblastoma cells.

References

1. Wang TH, Wang HS, Soong YK (2000) Paclitaxel-induced cell death: where the cell cycle and apoptosis come together. Cancer 88:2619–2628
2. Pendino F, Flexor M, Delhommeau F, Buet D, Lanotte M, Segal-Bendirdjian E (2001) Retinoids down regulate telomerase and telomere length in a pathway distinct from leukemia cell differentiation. Proc Natl Acad Sci USA 98:6662–6667
3. Dragnev KH, Rigas JR, Dmitrovsky E (2000) The retinoids and cancer prevention mechanisms. Oncologist 5:361–368
4. Thalasila A, Poplin E, Shih J, Dvorzhinski D, Capanna T, Doyle-Lindrud S, Beers S, Goodin S, Rubin E, DiPaola RS (2003) A phase I trial of weekly paclitaxel, 13-*cis* retinoic acid, and interferon-α in patients with prostate cancer and other advanced malignancies. Cancer Chemother Pharmacol 52:119–124
5. Vaishampayan U, Flaherty L, Du W, Hussain M (2001) Phase II evaluation of paclitaxel, α-interferon, and *cis*-retinoic acid in advanced renal cell carcinoma. Cancer 92:519–523
6. Yu C, Wang S, Dent P, Grant S (2001) Sequence-dependent potentiation of paclitaxel-mediated apoptosis in human leukemia cells by inhibitors of the mitogen-activated protein kinase kinase/mitogen-activated protein kinase pathway. Mol Pharmacol 60:143–154
7. Das A, Banik NL, Ray SK (2007) Garlic compounds generate reactive oxygen species leading to activation of stress kinases and cysteine proteases for apoptosis in human glioblastoma cells. Cancer 110:1083–1095
8. Das A, Sribnick EA, Wingrave JM, Wilford GG, Del Re AM, Woodward JJ, Appel SH, Banik NL, Ray SK (2005) Calpain activation in apoptosis of ventral spinal cord 4.1 (VSC4.1) motoneurons exposed to glutamate: Calpain inhibition provided functional neuroprotection. J Neurosci Res 81:551–562
9. Das A, Garner DP, Wilford GG, Del Re AM, Kumar DM, Woodward JJ, Banik NL, Agrawal N, Ray SK (2006) Calpeptin provides functional neuroprotection to rat retinal ganglion cells following Ca^{2+} influx. Brain Res 1084:146–157
10. Das A, Banik NL, Ray SK (2006) Mechanism of apoptosis with the involvement of proteolytic activities of calpain and caspases in human malignant neuroblastoma SH-SY5Y cells exposed to flavonoids. Int J Cancer 119:2575–2585
11. Kim NW, Piatyszek MA, Prowse KR, Harley CB, West MD, Ho PL, Coviello GM, Wright WE, Weinrich SL, Shay JW. (1994) Specific association of human telomerase activity with immortal cells and cancer. Science 66:2011–2015
12. Reid AB, Kurten RC, McCullough SS, Brock RW, Hinson JA (2005) Mechanisms of acetaminophen-induced hepatotoxicity: role of oxidative stress and mitochondrial permeability transition in freshly isolated mouse hepatocytes. J Pharmacol Exp Ther 312:509–516

13. Ray SK, Patel SJ, Welsh CT, Wilford GG, Hogan EL, Banik NL (2002) Molecular evidence of apoptotic death in malignant brain tumors including glioblastoma multiforme: upregulation of calpain and caspase-3. J Neurosci Res 69:197–206

14. Smiley ST, Reers M, Mottola-Hartshorn C, Lin M, Chen A, Smith TW, Steele GD Jr, Chen LB (1991) Intracellular heterogeneity in mitochondrial membrane potentials revealed by a J-aggregate-forming lipophilic cation JC-1. Proc Natl Acad Sci USA 88:3671–3675

15. Deissler H, Blass-Kampmann S, Bruyneel E, Mareel M, Rajewsky MF (1999) Neural cell surface differentiation antigen gp130 (RB13–6) induces fibroblasts and glioma cells to express astroglial proteins and invasive properties. FASEB J 13:657–666

16. Jakubowski W, Bartosz G (2000) 2,7-dichlorofluorescein oxidation and reactive oxygen species: what does it measure? Cell Biol Int 24:757–760

17. Aoshiba K, Yasui S, Nishimura K, Nagai A (1999) Thiol depletion induces apoptosis in cultured lung fibroblasts. Am J Respir Cell Mol Biol 21:54–64

18. Yamamoto K, Ichijo H, Korsmeyer SJ (1999) Bcl-2 is phosphorylated and inactivated by an ASK1/Jun N-terminal protein kinase pathway normally activated at G_2/M. Mol Cell Biol 19:8469–8478

19. Fan M, Du L, Stone AA, Gilbert KM, Chambers TC (2000) Modulation of mitogen-activated protein kinases and phosphorylation of Bcl-2 by vinblastine represent persistent forms of normal fluctuations at G2/M1. Cancer Res 60:6403–6407

20. Silke J, Vaux DL (2001) Two kinds of BIR-containing protein - inhibitors of apoptosis, or required for mitosis. J Cell Sci 114:1821–1827

21. Wingrave JM, Sribnick EA, Wilford GG, Matzelle DD, Mou JA, Ray SK, Hogan EL, Banik NL (2004) Higher calpastatin levels correlate with resistance to calpain-mediated proteolysis and neuronal apoptosis in juvenile rats after spinal cord injury. J Neurotrauma 21:1240–1254

22. Yuan Q, Ray RM, Johnson LR (2000) Polyamine depletion prevents camptothecin-induced apoptosis by inhibiting the release of cytochrome c. Am J Physiol Cell Physiol 282:C1290–C1297

23. Blagosklonny MV, Giannakakou P, Deiry WS, Kingston DG, Higgs PI, Neckers L, Fojo T (1997) Raf-1/Bcl-2 phosphorylation: a step from microtubule damage to cell death. Cancer Res 57:130–135

24. Kumanishi T, Usui H, Ichikawa T, Nishiyama A, Katagiri T, Abe S, Yoshida Y, Washiyama K, Kuwano R, Sakimura K (1992) Human glial fibrillary acidic protein (GFAP): molecular cloning of the complete cDNA sequence and chromosomal localization (chromosome 17) of the GFAP gene. Acta Neuropathol 83:569–578

25. Feng J, Funk WD, Wang S-S, Weinrich SL, Avilion AA, Chiu CP, Adams RR, Chang E, Allsopp RC, Yu J. (1995) The RNA component of human telomerase. Science 269:1236–1241

26. Meyerson M, Counter CM, Eaton EN, Ellisen LW, Steiner P, Caddle SD, Ziaugra L, Beijersbergen RL, Davidoff MJ, Liu Q, Bacchetti S, Haber DA, Weinberg RA (1997) hEST2, the putative human telomerase catalytic subunit gene, is upregulated in tumor cells and during immortalization. Cell 90:785–795